Structure of the Molybdenum Site of *Rhodobacter sphaeroides* Biotin Sulfoxide Reductase†

Carrie A. Temple,‡ Graham N. George,§ James C. Hilton,‡ Martin J. George,§ Roger C. Prince,|| Michael J. Barber,⊥ and K. V. Rajagopalan*,‡

Department of Biochemistry, Duke University Medical Center, Durham, North Carolina 27710, Stanford Synchrotron Radiation Laboratory, SLAC, Stanford University, P.O. Box 4349, MS 69, Stanford, California 94309, Exxon Research and Engineering Company, Route 22 East, Annandale, New Jersey 08801, and Department of Biochemistry and Molecular Biology, College of Medicine and H. Lee Moffitt Cancer Center and Research Institute, University of South Florida, Tampa, Florida 33612

Received September 17, 1999; Revised Manuscript Received December 23, 1999

ABSTRACT: Conditions for heterologous expression of *Rhodobacter sphaeroides* biotin sulfoxide reductase in *Escherichia coli* were modified, resulting in a significant improvement in the yield of recombinant enzyme and enabling structural studies of the molybdenum center. Quantitation of the guanine and the molybdenum as compared to that found in *R. sphaeroides* DMSO reductase demonstrated the presence of the bis(MGD)molybdenum cofactor. UV−visible absorption spectra were obtained for the oxidized, NADPH-reduced, and dithionite-reduced enzyme. EPR spectra were obtained for the Mo(V) state of the enzyme. X-ray absorption spectroscopy at the molybdenum K-edge has been used to probe the molybdenum coordination of the enzyme. The molybdenum site of the oxidized protein possesses a Mo(VI) mono-oxo site (Mo═O at 1.70 Å) with additional coordination by approximately four thiolate ligands at 2.41 Å and probably one oxygen or nitrogen at 1.95 Å. The NADPH- and dithionite-reduced Mo(IV) forms of the enzyme are des-oxo molybdenum sites with approximately four thiolates at 2.33 Å and two different Mo−O/N ligands at 2.19 and 1.94 Å.

Molybdenum enzymes catalyze a variety of two-electron redox reactions, many involving oxo group transfer (*1*). They can be divided into several groups based upon amino acid sequence similarities and the coordination environment of molybdenum (*1*). The dimethyl sulfoxide (DMSO)[1] reductase group contains the molybdopterin guanine dinucleotide (MGD) variant of the molybdenum cofactor. *Rhodobacter* DMSO reductase contains, as its sole prosthetic group, bis-(MGD)molybdenum in which the molybdenum atom is coordinated to four sulfur atoms from the dithiolenes of the two pterins as well as to serine 147 (*2*, *3*). There are several reported crystal structure studies of DMSO reductase from *Rhodobacter sphaeroides* (*3*) and *Rhodobacter capsulatus* (*4*−*6*), and all confirm the presence of the bis(MGD)-molybdenum form of the cofactor and show nearly identical folds for the polypeptide chain, plus a protein serine ligand on the metal. Despite these similarities, there are marked differences among the three structures in the details of molybdenum ligation, including disparities in the apparent number of Mo═O groups and the nature of the dithiolene linkage. All but one of the structures suggested from crystallographic data show chemically unusual features, with atoms in unusual positions and overly crowded active sites (*7*). The recent 2.5 Å crystal structure of *Shewanella massilia* trimethylamine *N*-oxide (TMAO) reductase shows essentially the same overall protein fold seen in DMSO reductase (*8*) and an active site that is clearly related to that of DMSO reductase. The molybdenum active site structure suggested by this study is also unusually crowded, and we note that the authors are careful to state that their data lack the resolution to definitively determine the metal coordination.

The structure of the molybdenum active site of *Rhodobacter* DMSO reductase has also been examined using extended X-ray absorption fine structure (EXAFS) spectroscopy on both wild type and recombinant *R. sphaeroides* protein (*7*, *9*). These show the presence of approximately four Mo−S ligands, one Mo−O known to arise from molybdenum ligation to serine 147, and unambiguously indicate that the Mo(VI) enzyme contains one terminal oxygen ligand (Mo═O). Reduction with dithionite or dimethyl sulfide (DMS) leads to the loss of the oxo group, generating a des-oxo molybdenum center. EXAFS analysis of *R. capsulatus* DMSO reductase (*10*) also indicates the presence of four Mo−S ligands and metal coordination to

† Research at Duke University was supported by Grant GM00091 from the National Institutes of Health. The Stanford Synchrotron Radiation Laboratory is funded by the Department of Energy, Office of Basic Energy Sciences. The Biotechnology Program is supported by the National Institutes of Health, Biomedical Research Technology Program, Division of Research Resources. Further support is provided by the Department of Energy, Office of Biological and Environmental Research.

* To whom correspondence should be addressed. Tel: (919) 681-8845; fax: (919) 684-8919; e-mail: raj@biochem.duke.edu.

‡ Duke University Medical Center.

§ Stanford University.

|| Exxon Research and Engineering Company.

⊥ University of South Florida.

[1] Abbreviations: DMSO, dimethyl sulfoxide; MGD, molybdopterin guanine dinucleotide; TMAO, trimethylamine *N*-oxide; BSO, biotin sulfoxide; EXAFS, extended X-ray absorption fine structure; EPR, electron paramagnetic resonance; XAS, X-ray absorption spectroscopy.

10.1021/bi9921541 CCC: $19.00
Published on Web 03/18/2000

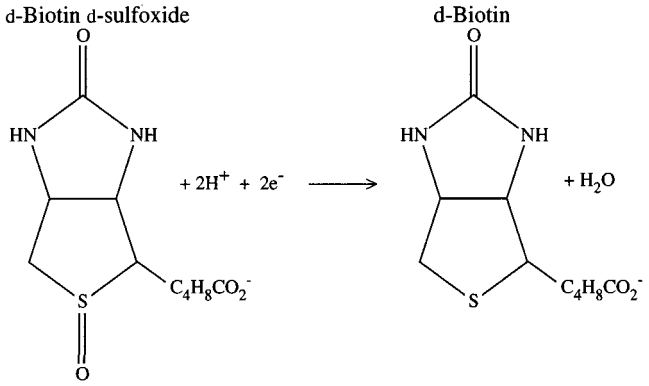

FIGURE 1: Primary reaction catalyzed by BSO reductase.

an oxygen atom presumably from serine; however, in disagreement with the *R. sphaeroides* results, the EXAFS analysis of Baugh et al. (*10*) suggested the presence of a second Mo−O bond in addition to the one terminal oxo group. For the enzyme in the DMS-reduced state, they argue for the presence of an oxo group as well as second Mo−O bond. A more recent EXAFS study (*7*) has pointed out flaws in the methods used by Baugh et al. (*10*) and suggested that their data are actually more consistent with the interpretation of the *R. sphaeroides* EXAFS (*7*, *9*).

One approach toward resolving the controversy surrounding the nature of the molybdenum coordination environment of *Rhodobacter* DMSO reductase is to study the active sites of closely related enzymes. Prokaryotic BSO reductase catalyzes the reduction of D-biotin D-sulfoxide (BSO) to D-biotin (Figure 1). Possible roles for the enzyme include scavenging BSO from the environment to generate biotin and protecting the cell from oxidative damage (*11*). Recently, Pollock and Barber successfully expressed *R. sphaeroides* BSO reductase in *Escherichia coli* (*12*, *13*). The enzyme was purified to homogeneity and used to demonstrate that BSO reductase possesses the molybdenum cofactor as the sole prosthetic group. In addition, they performed kinetic analysis of the enzyme with a variety of related substrates and demonstrated that the enzyme could directly utilize NADPH as a reducing agent (*13*).

Optimization of the expression conditions for *R. sphaeroides* BSO reductase now allows purification of sufficient enzyme for structural studies of the molybdenum site. Chemical analysis demonstrates the presence of the bis-(MGD)molybdenum form of the cofactor in BSO reductase. The enzyme has also been examined using UV−visible, X-ray absorption, and EPR spectroscopy. Since the enzymes in this group cycle between the Mo(VI) and the Mo(IV) oxidation states, with the Mo(VI) state donating the oxygen atom to the physiological acceptor (*1*), we have examined the oxidized, NADPH-reduced, and dithionite-reduced forms of *R. sphaeroides* BSO reductase.

EXPERIMENTAL PROCEDURES

Materials. Ultrafiltration devices and membranes were from Millipore. Q-Sepharose fast flow, Superose 12, and glutathione-agarose affinity resins as well as Factor Xa protease were obtained from Amersham Pharmacia Biotech. IPTG was obtained from Research Products International. All other reagents were obtained from Sigma.

Protein Expression and Purification. Wild type and recombinant *R. sphaeroides* DMSO reductase were purified as previously described (*14*). Recombinant BSO reductase was purified from *E. coli* JM109 cells transformed with the pGEX-5X-2 vector containing the BSO reductase sequence (*13*). Cells were grown aerobically at 37 °C overnight in an 80-mL culture containing LB supplemented with 100 μg/mL ampicillin. The mature overnight culture was divided equally between two 1-L cultures containing LB supplemented with ampicillin and 0.5 mM Na_2MoO_4 and subsequently grown aerobically at 30 °C until the $OD_{600} = 1$. Both 1-L cultures were used to inoculate a 40-L culture of M9ZB media supplemented as described previously (*14*) with 100 μg/mL ampicillin replacing all other antibiotics. Na_2MoO_4 was present at 1.0 mM, and IPTG was added to 40 μM. The cells were then grown anaerobically for 24 h at room temperature and harvested by centrifugation at 5000*g*.

The recombinant protein was purified in the absence of protease inhibitors following the general protocol previously described (*13*). A Microfluidics M110L microfluidizer processor was used instead of sonication. Cell lysis was achieved by three passages through a 112 μm interaction chamber at 16 000−18 000 psi. A 50-mL glutathione-agarose affinity column, a 24-mL Q-sepharose HR16/10 FPLC column, and a 100-mL Superose 12 HR16/50 FPLC column were used for the chromatographic steps. Factor Xa proteolysis was carried out at 4 °C.

Protein Analysis. The molybdenum and guanine content of the purified proteins were analyzed as described previously (*14*). Pure samples of *R. sphaeroides* DMSO reductase were quantitated spectrophotometrically at 280 nm using an extinction coefficient of 200 000 M^{-1} cm^{-1} or 2.3 $(mg/mL)^{-1}$ cm^{-1} (*2*). The concentration of both BSO reductase and total protein was determined using the Pierce BCA assay on trichloroacetic acid-precipitated samples as described in the manufacturer's protocol, with purified *R. sphaeroides* DMSO reductase as the standard.

UV−Visible Absorption Spectroscopy. Absorption spectroscopy was carried out using a Shimadzu UV-2101 PC spectrophotometer, and anaerobic samples were prepared in a Coy chamber containing a nitrogen, carbon dioxide, and hydrogen gas mix. All BSO reductase spectra were recorded in 50 mM Tris-HCl, pH 8.0, at an enzyme concentration greater than 5 mg/mL and subsequently normalized to 1 mg/mL for comparison of spectra. To obtain the NADPH-reduced BSO reductase spectrum, the enzyme was concentrated to approximately 100 μL and then diluted under anaerobic conditions with 800 μL of anaerobic buffer. The cuvette was then sealed, removed from the anaerobic environment, injected with 100 μL of 2.5 mM NADPH in an anaerobic buffer solution, and mixed gently by inversion before the spectrum was recorded. The reference spectrum of NADPH was obtained by an identical procedure in the absence of enzyme. For the dithionite-reduced spectrum, the protein was transferred to the cuvette under anaerobic conditions, and then the cuvette was sealed and removed from the anaerobic environment. Solid sodium dithionite was dissolved in an anaerobic buffer solution, and small amounts of this mixture were injected into the enzyme solution and mixed gently by inversion until the yellowish green color indicative of reduced enzyme was obtained. At this point, the reduced spectrum was recorded, and the injection of more

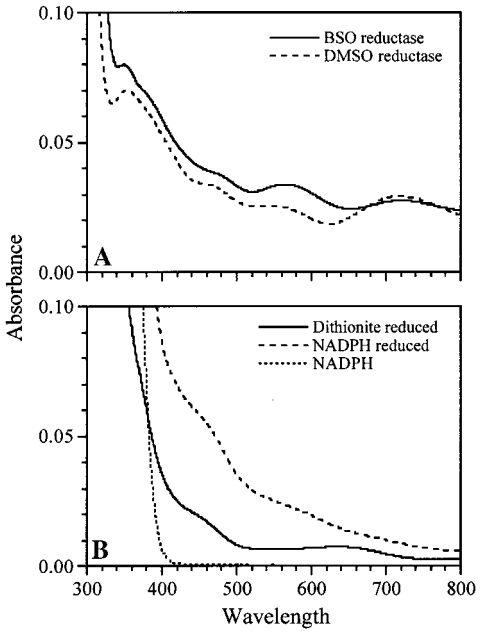

FIGURE 2: UV−visible absorption spectra of *R. sphaeroides* BSO reductase. (A) 1 mg/mL oxidized recombinant BSO reductase as compared to 1 mg/mL wild type *R. sphaeroides* DMSO reductase. (B) 1 mg/mL dithionite-reduced and NADPH-reduced BSO reductase with an equivalent spectrum of NADPH in the absence of enzyme.

dithionite did not change the spectrum. The *R. sphaeroides* DMSO reductase spectra shown in Figure 2 have been published previously (*14*).

EPR Spectroscopy. Mo(V) EPR spectra were recorded on a JEOL RE1X instrument at a sample temperature of 77 K, with other operating conditions identical to those described by George et al. (*7*). Unless otherwise stated, samples for Mo(V) EPR spectroscopy were prepared in quartz tubes (3 mm i.d.) by addition of an anaerobic solution of sodium dithionite under 1 atm of nitrogen to a final concentration of 1 mM and then quickly frozen by immersion of the tube in cold isopentane at −140 °C.

X-ray Absorption Spectroscopy. The enzyme was concentrated to approximately 2 mM molybdenum in 25 mM *N*-tris-[hydroxymethyl]methyl-2-aminoethanesulfonate, pH 8.0, and frozen in 10 × 10 × 3 mm Lucite sample cuvettes. Dithionite-reduced samples were prepared by adding an excess of an anaerobic dithionite solution containing trace methyl viologen to air-oxidized enzyme. The anaerobiosis of the sample was indicated by the persistence of the blue color of reduced methyl viologen. Reduction by NADPH was performed aerobically. XAS measurements were carried out at the Stanford Synchrotron Radiation Laboratory with the SPEAR storage ring containing 55−90 mA at 3.0 GeV. Molybdenum K-edge data were collected on beamline 7-3 using a Si(220) double crystal monochromator, with an upstream vertical aperture of 1 mm, and a wiggler field of 1.8 T. Harmonic rejection was accomplished by detuning one monochromator crystal to approximately 50% off peak, and no specular optics were present in the beamline. The incident X-ray intensity was monitored using an argon-filled ionization chamber, and X-ray absorption was measured as the X-ray molybdenum K_α fluorescence excitation spectrum using an array of 13 germanium intrinsic detectors (*15*). During data collection, samples were maintained at a temperature of approximately 10 K using an Oxford Instruments liquid helium flow cryostat. For each sample, six 30-min scans were accumulated, and the absorption of a molybdenum metal foil was measured simultaneously by transmittance. The energy was calibrated with reference to the lowest energy inflection point of the molybdenum foil, which was assumed to be 20 003.9 eV. The EXAFS oscillations $\chi(k)$ were quantitatively analyzed by curve-fitting using the EXAFSPAK suite of computer programs[2] as described by George et al. (*7*, *9*).

Table 1: Stoichiometry of the Structural Components of the Molybdenum Cofactor

	protein (μM)	Gua (μM)	Mo (μM)	Gua per protein	Mo per protein	Gua per Mo
BSO reductase	31.3	61.8	27.6	1.97	0.882	2.23
DMSO reductase	28.5	56.8	25.9	1.99	0.909	2.19

RESULTS

Optimization of Expression Conditions. Although Pollock and Barber were able to express active *R. sphaeroides* BSO reductase heterologously in *E. coli*, the expression level was low, yielding 0.125 mg of purified protein/L of culture (*13*). Utilizing the same expression vector and *E. coli* strain, a significant improvement in yield was obtained in these studies by modifying the expression conditions. By changing to anaerobic expression conditions in conjunction with a lower level of IPTG and a longer growth period, as much as 46 mg of purified enzyme could be obtained from a single 40-L anaerobic growth with 26% recovery and 120-fold purification. This represents an overall yield of 1.15 mg of protein/L of culture, a 9-fold increase over that previously described, and allows purification of sufficient enzyme for structural studies of the molybdenum center. The improvement in yield has also not compromised cofactor incorporation. The purified BSO reductase has a molybdenum content of at least 88%, and enzymatic activity is comparable to that observed following purification from the original expression conditions.

Stoichiometry of Cofactor Components. Qualitative analysis of *R. sphaeroides* BSO reductase has shown the presence of the MGD variant of the molybdenum cofactor (*13*); however, a complete cofactor characterization requires quantitative analysis, in view of the presence of the bis-(MGD)molybdenum form of the cofactor in other closely related enzymes including *R. sphaeroides* DMSO reductase. The molybdenum and guanine content of *R. sphaeroides* BSO reductase were determined and compared to that found in DMSO reductase (Table 1). The molar ratio of molybdenum to protein for BSO reductase was 0.882, with a guanine to protein ratio of 1.97 resulting in a guanine to molybdenum ratio of 2.33. This is comparable to a 2.19 ratio for DMSO reductase, demonstrating the presence of bis-(MGD)molybdenum in BSO reductase as well.

UV−Visible Absorption Spectroscopy. UV−visible absorption spectra were obtained of oxidized BSO reductase as well as enzyme reduced by dithionite or NADPH (Figure 2). The oxidized enzyme is dark brown, while the reduced enzyme is a light yellowish green. The broad spectral features resemble the pattern observed with *R. sphaeroides* DMSO

[2] http://ssrl.slac.stanford.edu/exafspak.html.

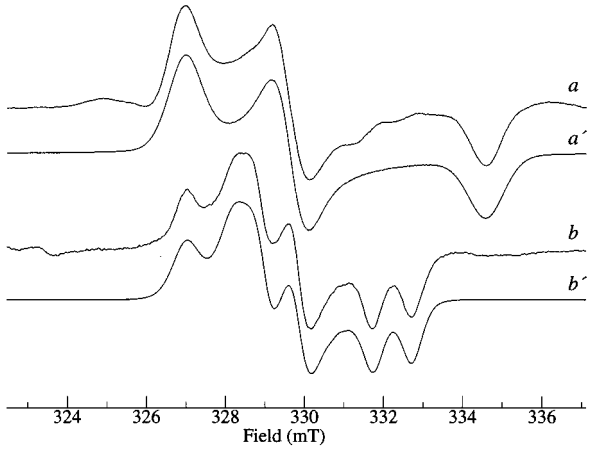

FIGURE 3: Mo(V) EPR spectra of *R. sphaeroides* BSO reductase and DMSO reductase in ^1H_2O. (a) and (b) show experimental spectra of BSO reductase and DMSO reductase, respectively. (a′) and (b′) show computer simulations of (a) and (b), respectively. These were calculated with the spin Hamiltonian parameters g_{xyz} = 1.9507, 1.9804, and 1.9962 and $A(^1H)_{xyz}$ = ∼2, ∼11, and ∼10 MHz (for BSO reductase) and g_{xyz} = 1.9645, 1.9813, and 1.9924 and $A(^1H)_{xyz}$ = 26.1, 24.5, and 33.3 MHz [for DMSO reductase (*7*)]. In the case of BSO reductase, the anisotropic coupling was estimated from the slight line-broadening observed in ^1H_2O, relative to that observed in ^2H_2O, and the ratio of nuclear *g* values, assuming only a single coupled proton.

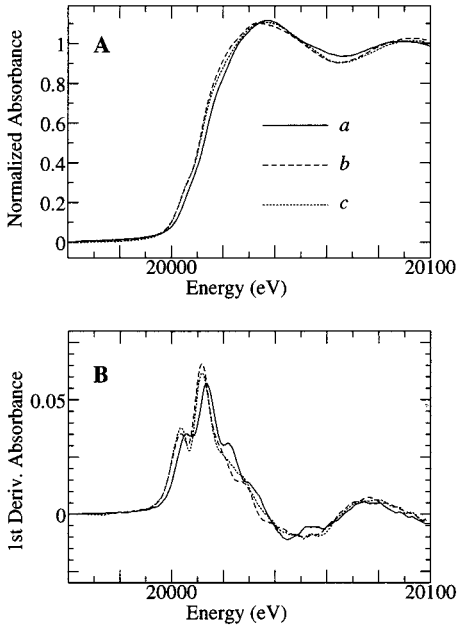

FIGURE 4: Molybdenum K-edge X-ray absorption near-edge spectra of BSO reductase (a) oxidized, as-isolated enzyme, (b) dithionite-reduced, and (c) NADPH-reduced enzyme.

reductase, indicating a similar ligand field for molybdenum (Figure 2A,). Unlike recombinant DMSO reductase (*7*, *14*), recombinant BSO reductase does not exhibit any large spectral differences or show any visible color change between the as-purified recombinant protein and the enzyme that has undergone one cycle of reduction followed by substrate reoxidation.[3] There are distinct differences in the long-wavelength regions of the reduced spectra depending upon the reductant used (Figure 2B), suggesting that the NADPH-reduced sample is a mixture of Mo(IV) and Mo(V), whereas the former species is predominant in the dithionite-reduced sample.

Mo(V) EPR Spectra. Figure 3 compares the Mo(V) EPR spectra of BSO reductase with that of DMSO reductase. Both samples were reduced for approximately 20 s with 1 mM (final) sodium dithionite solution and then rapidly frozen by immersion in a bath of cold isopentane at −140 °C. Enzyme before addition of exogenous reductant gave no EPR signals, which is consistent with the presence of fully oxidized Mo(VI). Longer exposure times to or higher concentrations of dithionite gave decreasing intensities of the Mo(V) EPR signal, suggesting more complete reduction to the EPR-silent Mo(IV) oxidation state. No Mo(V) EPR signals were observed when trace quantities of the mediator dye methyl viologen (∼4 μM) were included, suggesting complete reduction to the Mo(IV) oxidation state. Methyl viologen was added to the dithionite-reduced XAS samples (see below) to give fully reduced samples. The spectrum from BSO reductase lacks the resolved proton hyperfine observed for DMSO reductase and has rather broader line widths (Figure 3), greater *g*-anisotropy, and in particular, a significantly lower g_{xx}. Samples exchanged into ^2H_2O showed some sharpening of line widths (not illustrated), indicating the presence of unresolved anisotropic hyperfine interaction with at least one exchangeable proton.

Near-Edge X-Ray Absorption Spectra. The molybdenum K-edge spectra of oxidized, dithionite-reduced, and NADPH-reduced BSO reductase are broadly similar (Figure 4A), with subtle differences that are highlighted by the derivative plot (Figure 4B). The spectra of the reduced samples are shifted by approximately 1.5 eV to lower energy with respect to the spectrum of the oxidized sample. This is consistent with the expected oxidation states for molybdenum: Mo(VI) for oxidized and Mo(IV) for reduced. In contrast to the findings with recombinant DMSO reductase (*7*), the near-edge spectrum of BSO reductase first reduced with excess dithionite/methyl viologen and then reoxidized by turnover with a greater excess of biotin sulfoxide was found to be identical with that of the as-isolated oxidized enzyme.[3] None of the spectra have the pronounced pre-edge feature at about 20008 eV that has been observed in other molybdenum enzymes (*16*, *17*). This so-called oxo-edge feature is characteristic of a species possessing Mo═O groups (or to a lesser extent Mo═S), and it arises from formally dipole forbidden 1s → 4d bound-state transitions to antibonding orbitals directed principally along Mo═O bonds (*18*). The rather weak presence of this feature here argues for a low number (i.e., one or zero) of these ligands in the BSO reductase samples. Inspection of the derivative plots (Figure 4B) indicates that the spectra of the dithionite and the NADPH-reduced samples are subtly but significantly different, with the features of the latter spectrum being rather broader.

EXAFS Spectra. Figure 5 shows the EXAFS spectra, the best fits, and the corresponding Fourier transforms of BSO reductase in oxidized and reduced forms. The results of the curve-fitting analyses (Table 2) are fully consistent with a mono-oxo molybdenum site in the oxidized Mo(VI) enzyme similar to that observed for DMSO reductase (*7*, *9*) with a Mo═O bond length of 1.70 Å. The oxidized molybdenum site is also ligated by approximately four thiolate ligands,

[3] Data not shown.

Table 2: EXAFS Curve-Fitting Results[a]

	Mo═O			Mo−S			Mo−O			
sample	*N*	*R*	σ^2	*N*	*R*	σ^2	*N*	*R*	σ^2	error[b]
Mo(VI)	1	1.687(4)	0.0022(4)	3	2.405(1)	0.0024(1)				0.287
	1	1.686(4)	0.0026(4)	4	2.406(1)	0.0038(1)				0.280
	1	1.687(5)	0.0041(7)	5	2.407(1)	0.0051(2)				0.314
	1	**1.696(4)**	**0.0029(5)**	**4**	**2.406(1)**	**0.0038(1)**	**1**	**1.950(7)**	**0.0037(7)**	**0.234**[c]
	1	1.696(3)	0.0017[d]	4	2.406(1)	0.0038(1)	1	1.939(7)	0.0048(9)	0.239
	2	1.691(3)	0.0017[d]	4	2.407(2)	0.0037(2)				0.470
	2	1.702(3)	0.0017[d]	4	2.406(2)	0.0036(2)	1	1.895(8)	0.0022(8)	0.379
				4	2.406(2)	0.0039(2)				0.360
				4	2.406(2)	0.0040(2)	1	1.976(6)	0.0018(6)	0.348
Mo(IV)[f]				3	2.344(2)	0.0027(2)	1	2.161(9)	0.0010(9)	0.268
(NADPH)				4	2.335(2)	0.0047(3)	1	2.208(8)	0.0008(8)	0.263
				5	2.332(2)	0.0063(2)	1	2.216(6)	0.0001(6)	0.277
				4	**2.337(2)**	**0.0039(2)**	**1**	**1.909(9)**	**0.0053(8)**	**0.247**[c,e]
							1	**2.193(22)**	**0.0057(19)**	
Mo(IV)				3	2.338(2)	0.0015(1)	1	2.133(11)	0.0034(2)	0.223
(dithionite)				4	2.327(2)	0.0033(1)	1	2.232(18)	0.0019(2)	0.212
				5	2.342(1)	0.0039(2)	1	2.237(16)	0.0001(17)	0.227
				4	**2.333(2)**	**0.0030(1)**	**1**	**1.938(11)**	**0.0066(13)**	**0.198**[c]
							1	**2.185(26)**	**0.0070(14)**	

[a] Coordination number *N*, interatomic distance *R* (Å), and the (thermal and static) mean-square deviation in *R* (the Debye−Waller factor) σ^2 (Å^2). The values in parentheses are the estimated standard deviations (precisions) obtained from the diagonal elements of the covariance matrix. We note that the accuracies will always be somewhat larger than the precisions, typically ±0.02 Å for *R* and ±20% for *N* and σ^2. We also note that EXAFS cannot readily distinguish between scatterers of similar atomic number, such as chlorine and sulfur or nitrogen and oxygen. [b] The fit-error is defined as $\sum k^6(\chi_{exptl} - \chi_{calcd})^2/\sum k^6\chi_{exptl}^2$. [c] Fits shown in boldface represent the best fit obtained for the sample. [d] The value of σ^2 was restricted to a chemically reasonable value (0.0017 Å^2 for a Mo═O). [e] The improvement in the fit error upon introduction of a second Mo−O interaction is rather subtle, and we note that detection of the presence of this scatterer is correspondingly tentative. [f] Inclusion of Mo═O interactions in the Mo(IV) fits yielded unrealistically large values for σ^2, effectively removing this contribution from the fit.

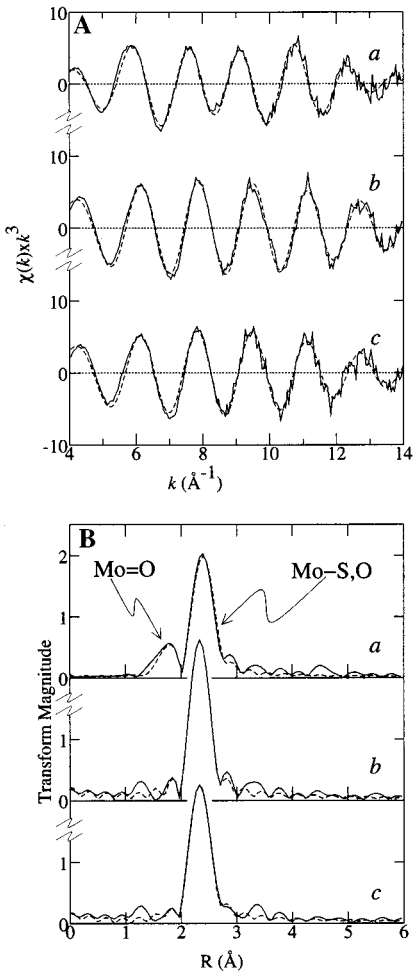

FIGURE 5: EXAFS curve-fitting results. (A) EXAFS spectra (solid lines) and best-fits (broken lines) of BSO reductase in (a) oxidized, (b) dithionite-reduced, and (c) NADPH-reduced forms. (B) EXAFS Fourier transforms phase-corrected for Mo−S backscattering.

with Mo−S bond lengths of 2.41 Å and probably a single Mo−O (or Mo−N) at 1.95 Å (Table 2). Unlike recombinant DMSO reductase, the EXAFS of redox-cycled BSO reductase was found to be identical with that of the as-isolated oxidized enzyme, indicating that the redox-conditioning observed with DMSO reductase (*7*, *14*) does not occur with BSO reductase. The EXAFS of both dithionite-reduced and NADPH-reduced BSO reductase indicates a des-oxo molybdenum site, with approximately four thiolate ligands at 2.33 Å (Table 2). The absence of Mo═O interactions is evident from the lack of a peak at about 1.7 Å in the EXAFS Fourier transform (Figure 5B). A significant improvement in the fit to the Mo(IV) BSO reductase EXAFS was achieved by including two different Mo−O/N interactions (Table 2), and it seems probable that one of these originates from a Mo−OH or Mo−OH_2 ligation arising from protonation of the Mo═O ligand of the oxidized enzyme. As was found with the near-edge spectra, the two reduced samples yielded EXAFS spectra that were subtly different. This is most noticeable as a relative lowering of intensity of the major Fourier transform peak of the NADPH-reduced data set (Figure 5B), and curve-fitting indicates that this originates in subtly different Mo−S and Mo−O distances and Debye−Waller factors, perhaps due to slightly different active site geometries.

From these results, and by analogy with other molybdenum enzymes, we can postulate an active site structure for oxidized and reduced BSO reductase. The presence of an amino acid ligand to the metal has been demonstrated in a variety of molybdoenzymes through X-ray crystallography and site-directed mutagenesis (*1*). The coordinating amino acid is serine in *Rhodobacter* DMSO reductase (*3*, *4*, *6*), cysteine in *E. coli* nitrate reductase (*19*), and selenocysteine in *E. coli* formate dehydrogenase (*20*, *21*). Amino acid sequence alignment of BSO reductase (*12*) with other

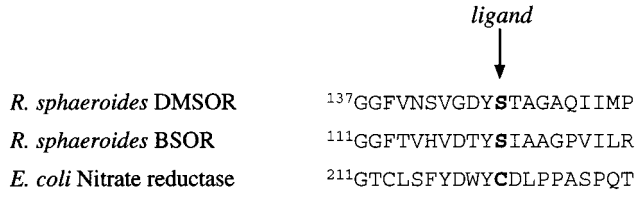

FIGURE 6: Comparison of aligned amino acid sequences at the molybdenum binding region of BSO reductase and related molybdenum enzymes.

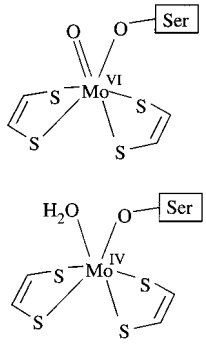

FIGURE 7: Proposed active site structures of the oxidized and reduced forms of BSO reductase. We note that EXAFS provides no direct information about geometry, and the structures postulated are thus tentative in this regard.

members of the DMSO reductase family of enzymes (*22*−*24*) indicates serine as the amino acid ligand to the molybdenum (Figure 6). We, therefore, postulate that one of the Mo−O ligands in the EXAFS curve-fitting is Mo−O−Ser[121]. The remainder of the metal coordination is completed by two cofactor dithiolene ligands and Mo═O in the fully oxidized enzyme, which should protonate to Mo−OH_2 in the reduced Mo(IV) enzyme, although Mo−OH is also possible (Figure 7). For the reduced enzyme, the shorter of the two Mo−O ligands is likely to be that from serine (Figure 7).

DISCUSSION

Optimization of conditions for recombinant expression of *R. sphaeroides* BSO reductase has resulted in the highest yield of a heterologously expressed molybdenum enzyme published to date, while reproducing the high percentage of cofactor incorporation previously observed with recombinant *R. sphaeroides* DMSO reductase (*14*). These results indicate that the traditional expression conditions may not result in the highest possible yield of molybdenum enzymes or other enzymes in which production of the cofactor is probably the limiting step in the expression of active enzyme. This increase in yield has made possible the purification of sufficient enzyme for structural studies of the molybdenum site.

According to the EXAFS curve-fitting analysis, oxidized BSO reductase possesses a Mo(VI) mono-oxo site with additional coordination by approximately four thiolate ligands and probably one oxygen or nitrogen. This is in agreement with quantitative analysis showing the presence of the bis-(MGD)molybdenum form of the cofactor and with serine 121 acting as the protein ligand to the molybdenum, as suggested from amino acid sequence alignment. The reduced Mo(IV) form of the enzyme is a des-oxo molybdenum site with approximately four thiolate and two different Mo−O/N ligands at 1.94 and 2.19 Å; the shorter bond likely arises from a Mo−O ligand to serine, while the longer bond probably results from protonation of the Mo═O of the fully oxidized enzyme to Mo−OH or Mo−OH_2. This analysis is in excellent agreement with the EXAFS of wild type and recombinant *R. sphaeroides* DMSO reductase in both the number and the types of molybdenum ligands observed, with the exception of the dithionite-reduced form of the enzyme, in which the best fit analysis indicated only three thiolate ligands with DMSO reductase but four in BSO reductase. The results presented herein, in conjunction with the recent EXAFS studies on *R. sphaeroides* DMSO reductase (*7*), indicate that the oxidized forms of at least two bis(MGD)-molybdenum-containing members of the DMSO reductase family of enzymes contain a mono-oxo Mo(VI) active site that converts to a des-oxo Mo(IV) site upon reduction.

The recent resonance Raman studies on *R. sphaeroides* DMSO reductase have corroborated the EXAFS data and have shown that an oxotransferase mechanism is consistent with a mono-oxo Mo(VI) and a des-oxo Mo(IV) state (*25*). The EXAFS structural data for BSO reductase support a very similar catalytic mechanism since both the oxidized and the reduced forms of BSO reductase show strong similarities to those of DMSO reductase. Quite recently, proof of direct oxygen atom transfer from the substrate to the enzyme has been obtained from resonance Raman studies on BSO reductase (*26*).

Unlike recombinant DMSO reductase, recombinant BSO reductase does not exhibit any large spectroscopic differences between the as-purified protein and the enzyme that has undergone one cycle of reduction followed by substrate oxidation. EXAFS studies on as-purified recombinant DMSO reductase (*7*) revealed a novel di-oxo coordination of the molybdenum center with apparently no coordinating amino acid side chain residue. Upon redox cycling, this form of DMSO reductase converts to a mono-oxo structure indistinguishable from the enzyme isolated from *R. sphaeroides*. This difference was attributed to the absence of the endogenous reductant of the enzyme and the lack of any catalytic turnover after formation of the holoenzyme (*14*). The presence of the mono-oxo functional active site in as-purified recombinant BSO reductase supports this hypothesis, since the recombinant expression conditions should expose BSO reductase to opportunities for redox cycling involving NADPH.

The similarity of the Mo K-edge EXAFS of BSO reductase to that of DMSO reductase argues for very similar active site structures, particularly for the oxidized enzymes. The striking similarity of the UV−visible spectra of the oxidized enzymes clearly reinforces this notion. In contrast, the Mo(V) EPR spectra of the two enzymes are significantly different. BSO reductase has much broader line widths, and the *g*-anisotropy is also greater, although well within the expected range for molybdenum enzymes. Since the terminal oxo group should convert to a hydroxyl group upon a one-electron reduction, the Mo(V) signal-giving species is likely to be a des-oxo structure. We have previously reviewed some factors that are important in determining *g*-anisotropy in des-oxo Mo(V) species (*7*), and in the absence of a Mo═O group, the EPR will be very sensitive to the geometry and the nature of the ligands. Thus, the differences in *g*-anisotropy could be the result of quite subtle geometric variations between

the active sites. The broader line widths of the BSO reductase Mo(V) EPR signal suggest an increased *g* strain, which might arise with increased solvent exposure of molybdenum site (although we note that this is far from definitive).

Both UV−visible and X-ray absorption spectroscopy indicate some differences between the dithionite- and the NADPH-reduced forms of BSO reductase. EXAFS curve-fitting analysis indicates subtle differences in Mo−S and Mo−O distances and Debye−Waller factors between the two reduced forms. This may be due to a small amount of Mo(V) in the sample (i.e., the NADPH-reduced sample was actually a mixture of Mo(IV) and Mo(V) forms), which is suggested by the observation of a small amount of Mo(V) in EPR controls. Although analysis of EXAFS of mixtures can be problematic, our results do suggest that the Mo(V) and Mo(IV) forms have similar structures.

Amino acid sequence comparisons of BSO and DMSO reductase from *R. sphaeroides* previously revealed 50% sequence identity between the two enzymes (*12*). The results presented herein demonstrate that both enzymes contain the bis(MGD)molybdenum cofactor, and there are no large differences in the molybdenum coordination environment of the two enzymes. Therefore, subtle changes in the amino acid sequences must be responsible for the differences in substrate specificity as well as in the ability of BSO reductase to utilize NADPH as a reducing agent. DMSO and TMAO reductase utilize a membrane-bound cytochrome as the electron donor; BSO reductase is not a terminal respiratory electron acceptor and, indeed, is the only known enzyme in which NADPH serves as a direct reductant of the molybdenum center. Further research is required to determine the site of NADPH reduction, and detailed analysis of the interaction of NADPH with the molybdenum center should reveal whether the reduction involves direct transfer of a hydride ion to the molybdenum coordination sphere.

ACKNOWLEDGMENT

We are indebted to Ingrid J. Pickering of SSRL for assistance with data collection and Ralph Wiley of Duke University for assistance in enzyme purification.

REFERENCES

1. Kisker, C., Schindelin, H., and Rees, D. C. (1997) *Annu. Rev. Biochem. 66*, 233−267.
2. Hilton, J. C., and Rajagopalan, K. V. (1996) *Arch. Biochem. Biophys. 325*, 139−143.
3. Schindelin, H., Kisker, C., Hilton, J., Rajagopalan, K. V., and Rees, D. C. (1996) *Science 272*, 1615−1621.
4. Schneider, F., Löwe, J., Huber, R., Schindelin, H., Kisker, C., and Knäblein, J. (1996) *J. Mol. Biol. 263*, 53−69.
5. McAlpine, A. S., McEwan, A. G., Shaw, A. L., and Bailey, S. (1997) *J. Biol. Inorg. Chem. 2*, 690−701.
6. McAlpine, A. S., McEwan, A. G., and Bailey, S. (1998) *J. Mol. Biol. 275*, 613−623.
7. George, G. N., Hilton, J., Temple, C., Prince, R. C., and Rajagopalan, K. V. (1999) *J. Am. Chem. Soc. 121*, 1256−1266.
8. Czjzek, M., Dos Santos, J.-P., Pommier, J., Giordano, G., Mejean, V., and Haser, R. (1998) *J. Mol. Biol. 284*, 435−447.
9. George, G. N., Hilton, J., and Rajagopalan, K. V. (1996) *J. Am. Chem. Soc. 118*, 1113−1117.
10. Baugh, P. E., Garner, C. D., Charnock, J. M., Collison, D., Davies, E. S., McAlpine, A. S., Bailey, S., Lane, I., Hanson, G. R., and McEwan, A. G. (1997) *J. Biol. Inorg. Chem. 2*, 634−643.
11. Pierson, D. E., and Campbell, A. (1990) *J. Bacteriol. 172*, 2194−2198.
12. Pollock, V. V., and Barber, M. J. (1995) *Arch. Biochem. Biophys. 318*, 322−332.
13. Pollock, V. V., and Barber, M. J. (1997) *J. Biol. Chem. 272*, 3355−3362.
14. Hilton, J. C., Temple, C. A., and Rajagopalan, K. V. (1999) *J. Biol. Chem. 274*, 8428−8436.
15. Cramer, S. P., Tench, O., Yocum, M., and George, G. N. (1988) *Nucl. Instrum. Methods Phys. Res. A266*, 586−591.
16. George, G. N., Garrett, R. M., Prince, R. C., and Rajagopalan, K. V. (1996) *J. Am. Chem. Soc. 118*, 8588−8592.
17. George, G. N., Colangelo, C. M., Dong, J., Scott, R. A., Khangulov, S. V., Gladyshev, V. N., and Stadtman, T. C. (1998) *J. Am. Chem. Soc. 120*, 1267−1273.
18. Kutzler, F. W., Natoli, C. R., Misemer, D. K., Doniach, S., and Hodgson, K. O. (1980) *J. Chem. Phys. 73*, 3274−3288.
19. Barber, M. J., and Neame, P. J. (1990) *J. Biol. Chem. 34*, 20912−20915.
20. Gladyshev, V. N., Khangulov, S. V., Axley, M. J., and Stadtman, T. C. (1994) *Proc. Natl. Acad. Sci. U.S.A. 91*, 7708−7711.
21. Boyington, J. C., Gladyshev, V. N., Khangulov, S. V., Stadtman, T. C., and Sun, P. D. (1997) *Science 275*, 1305−1308.
22. Hilton, J. C., and Rajagopalan, K. V. (1996) *Biochim. Biophys. Acta 1294*, 111−114.
23. Blasco, F., Iobbi, C., Giordano, G., Chippaux, M., and Bonnefoy, V. (1989) *Mol. Gen. Genet. 218*, 249−256.
24. Zinoni, F., Birkmann, A., Stadtman, T. C., and Bock, A. (1986) *Proc. Natl. Acad. Sci. U.S.A. 83*, 4650−4654.
25. Garton, S. D., Hilton, J. C., Oku, H., Crouse, B. R., Rajagopalan, K. V., and Johnson, M. K. (1997) *J. Am. Chem. Soc. 119*, 12906−12916.
26. Garton, S. D., Temple, C. A., Dhawan, I. K., Barber, M. J., Rajagopalan, K. V., and Johnson, M. K. (2000) *J. Biol. Chem. 275*, 6798−6805.

BI9921541